Available online at www.sciencedirect.com
ScienceDirect
Acta Mathematica Scientia 2014,**34B**(5):1–19
Acta Mathematica Scientia 数学物理学报
http://actams.wipm.ac.cn

SPACE-TIME DISCONTINUOUS GALERKIN METHOD FOR MAXWELL EQUATIONS IN DISPERSIVE MEDIA*

Bo WANG (汪波) *Ziqing XIE* (谢资清)
College of Mathematics and Computer Science, and Key Laboratory of High Performance Computing and Stochastic Information Processing (Ministry of Education of China), Hunan Normal University, Changsha, Hunan 410081, China
E-mail: *bowanghn@gmail.com; ziqingxie@yahoo.com.cn*

Zhimin ZHANG (张智民)
Beijing Computational Science Research Center, Beijing 100084, China, and Department of Mathematics, Wayne State University, Detroit, MI 48202, USA
E-mail: *ag7761@wayne.edu*

Abstract In this paper, a unified model for time-dependent Maxwell equations in dispersive media is considered. The space-time DG method developed in [29] is applied to solve the underlying problem. Unconditional L^2-stability and error estimate of order $O(\tau^{r+1}+h^{k+1/2})$ is obtained when polynomials of degree at most r and k are used for the temporal discretization and spatial discretization respectively. 2-D and 3-D numerical examples are given to validate the theoretical results. Moreover, numerical results show an ultra-convergence of order $2r+1$ in temporal variable t.

Key words maxwell equations; dispersive media; space-time DG method; L^2-stability; L^2-error estimate

2010 MR Subject Classification 65N30; 65M60; 78M10

1 Introduction

In computational electromagnetics (CEM), constructing high order and efficient numerical scheme for solving time-dependent Maxwell equations is a very important research area. The first numerical method for time-dependent Maxwell's equations is the finite Difference time domain (FDTD) scheme, which was proposed by Yee in 1966 [30]. This scheme remains popular up to now due to its simplicity and efficiency. However, like most finite difference methods, the FDTD method has disadvantages in handling complex geometry and extending to high order scheme.

*Received October 28, 2013; revised January 10, 2014. The second author is supported by NSFC (11171104, 10871066) and the Construct Program of the Key Discipline in Hunan. The third author is supported in part by US National Science Foundation under Grant DMS-1115530

Instead, finite element methods can overcome these disadvantages. Thus they have been widely used to discretize Maxwell equations in recent years, e.g., conforming finite element methods including edge finite element method [8, 22, 25], node-based formulation [14], mixed finite element methods [16–19, 24] and discontinuous Galerkin finite element methods (DGFEMs) [7, 9, 12, 20]. In these methods, the spatial domain is discretized using finite element methods, producing a system of ordinary differential equations in time which in turn is discretized using finite difference methods or Runge-Kutta methods. Theoretical analysis was first given for semi-discrete scheme in which only the spatial domain was discretized [9, 24]. A fully discrete finite element method for solving Maxwell equations was analyzed by Makridakis and Monk in [23] in which the first order coupled system of electric field and magnetic field was considered. Then Ciarlet. Jr and Zou [8] developed a fully discrete finite element approach for the second order electric field equation, which was derived from Maxwell equations by eliminating the magnetic field. Both optimal energy-norm error estimate and L^2-norm error estimate were obtained.

Nevertheless, finite element methods have not been used to discretize the temporal domain of Maxwell equations in the works mentioned above, though finite element methods for temporal discretization are considered for some problems. Actually, it was first proposed by Argyris and Scharpf [1], Fried [11] and Oden [26] for solving dynamic problems. Since then the space-time finite element methods have been widely used to solve a variety of differential equations. See [2, 3, 5, 13] for the implementation of time-continuous Galerkin finite element schemes. On the other hand, the time-discontinuous Galerkin methods were originally developed for the first order hyperbolic equations [15, 27]. As a matter of fact, the time-discontinuous Galerkin framework seems conducive for the rigorous justification of the error estimates [21].

Motivated by these works, we proposed a space-time DG method for time-dependent Maxwell equations in simple media [29]. In this fully discrete DG formulation, DG method is used to discretize the spatial domain as well as the temporal domain. We showed that, compared to other numerical methods, this method has some advantages in the following aspects:

- Unconditional stability. Unlike some explicit numerical schemes, such as Runge-Kutta DG method (RKDG), which has a so-called CFL condition on the mesh size, this method is unconditionally stable. The algorithm works well even when the time step size τ is much larger than the spatial mesh size h.
- Rigorous and clear theoretical analysis. Since DG method is used to discretize the temporal domain as well as the spatial domain, many wonderful orthogonal properties can be used in the theoretical analysis, and then the proof is simplified significantly.
- High order convergence rate in both temporal domain and spatial domain. To our knowledge, most works on fully discrete numerical methods for Maxwell equations are based on the combination of finite difference method and finite element method. Thus, it is not easy to obtain a high order convergence rate in t. However, for our space-time DG method, it is very convenient to obtain high order convergence rate both in t and $\mathbf{x}$. In fact, we can prove the L^2-error estimate of order $O(\tau^{r+1} + h^{k+\frac{1}{2}})$.
- Ultra-convergence in temporal variable t. Numerical results show an ultra-convergence of order $2r+1$ in t when polynomials of degree at most r is used for temporal discretization.

In this paper, we would like to investigate the space-time DG method for solving Maxwell

equations when dispersive media are involved. Fully discrete finite element method for solving Maxwell equations in dispersive media was first studied by J. C. Li [16–19]. In these works, some important kinds of dispersive media e.g., cold plasma, Debye medium, Lorentz medium, and double negative metamaterials, were considered. A mixed finite element method was used to discretize the spatial domain and finite difference method for the temporal domain. Error estimates in both L^2 norm and energy norm were obtained. A study of RKDG method for solving time-dependent Maxwell equations in dispersive media can be found in [20] . Instead of finite difference method and Runge-Kutta method, DG method is used for the temporal discretization in our space-time DG method. We consider a unified model proposed in [28]. Unconditional L^2-stability is proved first. Moreover, an L^2-error estimate of order $O(\tau^{r+1} + h^{k+\frac{1}{2}})$ is obtained when polynomials of degree at most r and k are used for the temporal discretization and spatial discretization, respectively.

The outline of this paper is as follows. In Section 2, we introduce the model problem and its corresponding space-time DG scheme. In Section 3, L^2-stability and error estimates of our approach are discussed. In Section 4, numerical results are given to validate our theoretical prediction. Possible future work and concluding remarks are presented in Section 5.

2 Model Problem and Space-time DG Scheme

2.1 Model problem

We consider the following model

$$\mu\frac{\partial \mathbf{H}}{\partial t} + \nabla \times \mathbf{E} = 0 \qquad \text{in} \quad \Omega \times (0,T], \tag{2.1}$$

$$\epsilon\frac{\partial \mathbf{E}}{\partial t} - \nabla \times \mathbf{H} + \mathbf{J}(\mathbf{E},t) = 0 \qquad \text{in} \quad \Omega \times (0,T], \tag{2.2}$$

where Ω is a Lipchitz domain in R^2 or R^3, μ and ϵ are positive constants, and $\mathbf{J}$ is the so called polarization currents

$$\mathbf{J}(\mathbf{E},t) = c\mathbf{E} + \int_0^t \tilde{\kappa}(t-s)\mathbf{E}(\mathbf{x},s)\mathrm{d}s \tag{2.3}$$

with c a nonnegative constant and $\tilde{\kappa}$ a given function. This model was firstly introduced in [28] to unify some similar models which describe the electromagnetic wave propagation in some specific kinds of dispersive media (cold plasma, Debye medium, Lorentz medium, etc).

For simplicity, a perfect conduct boundary condition

$$\mathbf{n} \times \mathbf{E} = 0 \qquad \text{on} \quad \partial\Omega \times (0,T], \tag{2.4}$$

and a simple initial condition

$$\mathbf{E}(\mathbf{x},0) = \mathbf{E}_0(\mathbf{x}), \qquad \mathbf{H}(\mathbf{x},0) = \mathbf{H}_0(\mathbf{x}) \qquad \text{in} \quad \Omega, \tag{2.5}$$

are imposed, where $\mathbf{E}_0$ and $\mathbf{H}_0$ are given functions with $\mathbf{H}_0$ satisfying

$$\nabla \cdot (\mu\mathbf{H}_0) = 0 \qquad \text{in} \quad \Omega, \qquad \mathbf{H}_0 \cdot \mathbf{n} = 0 \qquad \text{on} \quad \partial\Omega. \tag{2.6}$$

To define our space-time DG scheme, we rewrite(2.1), (2.2) and (2.5) into the form

$$\mathbf{Q}\tilde{\mathbf{U}}_t + \nabla \cdot \mathbf{f}(\tilde{\mathbf{U}}) + \tilde{\mathbf{J}}(\tilde{\mathbf{U}}) = 0 \qquad \text{in} \quad \Omega \times (0,T], \tag{2.7}$$

$$\tilde{\mathbf{U}}(\mathbf{x},0)=\tilde{\mathbf{U}}_0(\mathbf{x}) \qquad \text{in } \ \Omega, \tag{2.8}$$

where

$$\tilde{\mathbf{U}}=\begin{pmatrix}\mathbf{H}\\ \mathbf{E}\end{pmatrix}, \quad \tilde{\mathbf{U}}_0=\begin{pmatrix}\mathbf{H}_0\\ \mathbf{E}_0\end{pmatrix}, \quad \mathbf{Q}=\begin{pmatrix}\mu I_{3\times 3} & 0_{3\times 3}\\ 0_{3\times 3} & \epsilon I_{3\times 3}\end{pmatrix},$$

and

$$\mathbf{f}(\tilde{\mathbf{U}})=[\mathbf{f}_1(\tilde{\mathbf{U}}),\mathbf{f}_2(\tilde{\mathbf{U}}),\mathbf{f}_3(\tilde{\mathbf{U}})]^T, \quad \mathbf{f}_i(\tilde{\mathbf{U}})=\begin{pmatrix}\mathbf{e}_i\times\mathbf{E}\\ -\mathbf{e}_i\times\mathbf{H}\end{pmatrix}, \quad \tilde{\mathbf{J}}(\tilde{\mathbf{U}})=\begin{pmatrix}0_{3\times 1}\\ \mathbf{J}(\mathbf{E},t)\end{pmatrix}.$$

On behalf of the theoretical analysis, we introduce a transform to produce a new term only depend on $\mathbf{U}$ in the Eq. (2.7). This new term plays a key role in the proof of L^2-stability as well as error estimate. For this purpose, let $\tilde{\mathbf{U}}=\mathrm{e}^{\lambda t}\mathbf{U}$, where λ is a positive real number. Then we have

$$\mathbf{U}\equiv\begin{pmatrix}\mathbf{H}^{\lambda}\\ \mathbf{E}^{\lambda}\end{pmatrix}=\begin{pmatrix}\mathrm{e}^{-\lambda t}\mathbf{H}\\ \mathrm{e}^{-\lambda t}\mathbf{E}\end{pmatrix}, \quad \frac{\partial\tilde{\mathbf{U}}}{\partial t}=\lambda\mathrm{e}^{\lambda t}\mathbf{U}+\mathrm{e}^{\lambda t}\frac{\partial\mathbf{U}}{\partial t}. \tag{2.9}$$

Denoted by

$$\mathbf{G}(\mathbf{E},t)=c\mathbf{E}+\int_0^t\kappa(t-s)\mathbf{E}(\mathbf{x},s)\mathrm{d}s, \quad \tilde{\mathbf{G}}(\mathbf{U})=\begin{pmatrix}0_{3\times 1}\\ \mathbf{G}(\mathbf{E}^{\lambda},t)\end{pmatrix}, \tag{2.10}$$

where $\kappa(t)=\tilde{\kappa}(t)\mathrm{e}^{-\lambda t}$, then (2.7)-(2.8) is equivalent to

$$\mathbf{Q}\mathbf{U}_t+\lambda\mathbf{Q}\mathbf{U}+\nabla\cdot\mathbf{f}(\mathbf{U})+\tilde{\mathbf{G}}(\mathbf{U})=0 \tag{2.11}$$

$$\mathbf{U}(\mathbf{x},0)=\tilde{\mathbf{U}}_0(\mathbf{x}). \tag{2.12}$$

It is worthwhile to point out that the space-time DG scheme is based on (2.11)–(2.12).

2.2 Space-time DG scheme

Assuming that $\mathcal{T}_h$ is a triangulation of the domain Ω with the element being denoted by K, the face by e, $h=min_K\{\text{the radius of the largest circle within } K\}$, and the outward normal by $\mathbf{n}_K$. We also denoted by $\mathcal{E}_{\mathcal{I}}$ the union of all interior faces of $\mathcal{T}_h$, by $\mathcal{E}_{\mathcal{D}}$ the union of all the boundary faces of $\mathcal{T}_h$, and by $\mathcal{E}=\mathcal{E}_{\mathcal{I}}\bigcup\mathcal{E}_{\mathcal{D}}$ the union of all faces of $\mathcal{T}_h$. Let $\mathcal{I}_h: 0=t_0<t_1<\cdots<t_n=T$ be a uniform subdivision of the interval $I=[0,T]$ with elements denoted by $I_j=[t_j,t_{j+1}]$ and time step size by $\tau=t_{j+1}-t_j$.

Let $P^k(K)$ denotes the space of polynomials with degree at most k. Then the DG finite element space for the spatial discretization is given by

$$\mathbf{S}_{h,\Omega}^k=\{v\in L^2(\Omega): v|_K\in\mathcal{P}^k(K), K\in\mathcal{T}_h\}.$$

On the other hand, define the DG finite element space for the temporal discretization:

$$\mathbf{S}_{h,I}^r=\{\mathbf{v}\in L^2(I): \mathbf{v}|_{I_j}\in\mathcal{P}^r(I_j), j=0,1,\cdots,n-1\}.$$

Finally, we define the discontinuous finite element space as follow

$$\mathbf{V}_h^{r,k}=\bar{\mathbf{V}}_h^{r,k}\oplus\bar{\mathbf{V}}_h^{r,k},$$

where

$$\bar{\mathbf{V}}_h^{r,k}=\left(\mathbf{S}_{h,I}^r\otimes\mathbf{S}_{h,\Omega}^k\right)^3.$$

In fact, each component of an element in $\bar{\mathbf{V}}_h^{r,k}$ is the product of two elements from $\mathbf{S}_{h,\Omega}^k$ and $\mathbf{S}_{h,I}^r$.

Defining the numerical flux is very important for the construction of a DG scheme. For the definition of numerical flux, we need to introduce some notations first. Let e be an interior face belonging to element K, and define

$$\mathbf{v}^{\mathrm{int}(K)}(\mathbf{x}) = \lim_{\delta\to 0-} \mathbf{v}(\mathbf{x}+\delta\mathbf{n}_K), \qquad \mathbf{v}^{\mathrm{ext}(K)}(\mathbf{x}) = \lim_{\delta\to 0+} \mathbf{v}(\mathbf{x}+\delta\mathbf{n}_K) \quad \forall \mathbf{x}\in e.$$

Then we define the average and tangential jump of $\mathbf{v}$ on any interior face e as follows:

$$\bar{\mathbf{v}} = \frac{\mathbf{v}^{\mathrm{int}(K)} + \mathbf{v}^{\mathrm{ext}(K)}}{2}, \quad [\![\mathbf{v}]\!]_T = \mathbf{n}_K \times \mathbf{v}^{\mathrm{int}(K)} - \mathbf{n}_K \times \mathbf{v}^{\mathrm{ext}(K)}.$$

For a boundary face $e \subset \mathcal{E}_{\mathcal{D}}$ which belongs to element K, we define

$$\mathbf{v}^{\mathrm{int}}(\mathbf{x}) = \mathbf{v}^{\mathrm{int}(K)}(\mathbf{x}), \qquad \forall \mathbf{x}\in e.$$

In addition, we define $\mathbf{v}(t_j^+) = \lim_{t\to t_j+0} \mathbf{v}(t), \mathbf{v}(t_j^-) = \lim_{t\to t_j-0} \mathbf{v}(t)$.

Now, we are ready for the definition of our space-time DG scheme. Multiplying (2.11)-(2.12) by test function $\mathbf{v} = [\mathbf{v}_H, \mathbf{v}_E]^T$ and integrating by parts over $Q_j^K = K \times I_j$, we obtain the weak formulation:

$$\begin{aligned} &-\int_{I_j}\int_K \mathbf{QU}\cdot\mathbf{v}_t \mathrm{d}\mathbf{x}\mathrm{d}t + \lambda\int_{I_j}\int_K \mathbf{QU}\cdot\mathbf{v}\mathrm{d}\mathbf{x}\mathrm{d}t + \int_{I_j}\int_{\partial K} (\mathbf{f}(\mathbf{U})\cdot\mathbf{n}_K)\cdot\mathbf{v}\mathrm{d}s\mathrm{d}t \\ &\quad -\int_{I_j}\int_K \mathbf{f}(\mathbf{U})\cdot\nabla\mathbf{v}\mathrm{d}\mathbf{x}\mathrm{d}t + \int_{I_j}\int_K \tilde{\mathbf{G}}(\mathbf{U})\cdot\mathbf{v}\mathrm{d}\mathbf{x}\mathrm{d}t + \int_K (\mathbf{QU}\cdot\mathbf{v})\,|_{t_j}^{t_{j+1}}\mathrm{d}\mathbf{x} = 0, \end{aligned} \tag{2.13}$$

Our space-time DG scheme based on weak formulation (2.13) is to find $\mathbf{U}_h \equiv (\mathbf{H}_h^\lambda, \mathbf{E}_h^\lambda)^T \in \mathbf{V}_h^{r,k}$, such that

$$\begin{aligned} &-\int_{I_j}\int_K \mathbf{QU}_h\cdot\frac{\partial}{\partial t}\mathbf{v}_h\mathrm{d}\mathbf{x}\mathrm{d}t + \lambda\int_{I_j}\int_K \mathbf{QU}_h\cdot\mathbf{v}_h\mathrm{d}\mathbf{x}\mathrm{d}t + \int_{I_j}\sum_{e\in\partial K}\int_e (\widehat{\mathbf{f}(\mathbf{U}_h)\cdot\mathbf{n}_K})\cdot\mathbf{v}_h\mathrm{d}s\mathrm{d}t \\ &-\int_{I_j}\int_K \mathbf{f}(\mathbf{U}_h)\cdot\nabla\mathbf{v}_h\mathrm{d}\mathbf{x}\mathrm{d}t + \int_{I_j}\int_K \tilde{\mathbf{G}}(\mathbf{U}_h)\cdot\mathbf{v}_h\mathrm{d}\mathbf{x}\mathrm{d}t + \int_K \big(\mathbf{Q}\hat{\mathbf{U}}_h\cdot\mathbf{v}_h\big)|_{t_j}^{t_{j+1}}\mathrm{d}\mathbf{x} = 0 \end{aligned} \tag{2.14}$$

for all $\mathbf{v}_h \in \mathbf{V}_h^{r,k}$ and all elements $Q_j^K = K\times I_j, K\in\mathcal{T}_h, j = 0,1,\cdots,n-1$. Here $(\widehat{\mathbf{f}(\mathbf{U}_h)\cdot\mathbf{n}_K})$ and $\hat{\mathbf{U}}_h$ are the numerical fluxes on the face $e\subset\mathcal{E}$ and the node point $t_j, j = 0,1,\cdots,n$, respectively. We take

$$\widehat{\mathbf{f}(\mathbf{U}_h)\cdot\mathbf{n}}_K = \begin{pmatrix} \mathbf{n}_K\times(\bar{\mathbf{E}}_h^\lambda - \frac{Z}{2}[\![\mathbf{H}_h^\lambda]\!]_T) \\ -\mathbf{n}_K\times(\bar{\mathbf{H}}_h^\lambda + \frac{1}{2Z}[\![\mathbf{E}_h^\lambda]\!]_T) \end{pmatrix} \tag{2.15}$$

on an interior face $e = \partial K\bigcap\mathcal{E}_I$ and

$$\widehat{\mathbf{f}(\mathbf{U}_h)\cdot\mathbf{n}} = \begin{pmatrix} \mathbf{0}_{3\times 1} \\ -\mathbf{n}\times\big[(\mathbf{H}_h^\lambda)^{\mathrm{int}} + \frac{1}{Z}\mathbf{n}\times(\mathbf{E}_h^\lambda)^{\mathrm{int}}\big] \end{pmatrix} \tag{2.16}$$

on a boundary face $e = \partial K\bigcap\mathcal{E}_D$, where $Z = \sqrt{\frac{\mu}{\epsilon}}$ denotes the impedance of the medium. Obviously this numerical flux is consistent with $\mathbf{f}(\mathbf{U})\cdot\mathbf{n}_K$. On the other hand, we take

$$\hat{\mathbf{U}}_h(\mathbf{x},t_j) = \mathbf{U}_h(\mathbf{x},t_j^-), \quad j = 1,2,\cdots,n, \quad \hat{\mathbf{U}}_h(\mathbf{x},0) = \mathbb{P}_h\mathbf{U}_0, \tag{2.17}$$

where $\mathbb{P}_h$ is the element-wise L^2 projection operator and will be defined later.

3 L^2-stability and Error Estimates

In this section, both the L^2-stability and error estimates are analyzed. The following notations for broken Sobolev spaces will be used in our theoretical analysis. Let $H^k(\Omega)$ and $H^k(I)$ denotes the standard Sobolev spaces with norms $\|\cdot\|_{k,\Omega}$ and $\|\cdot\|_{k,I}$. Then, we define the broken Sobolev spaces:

$$H^k(\mathcal{T}_h)=\Big\{u\Big|u|_K\in H^k(K),\ \forall K\in\mathcal{T}_h \text{ and } \sum_{K\in\mathcal{T}_h}||u||^2_{k,K}<\infty\Big\}, \tag{3.1}$$

and

$$H^k(\mathcal{I}_h)=\Big\{u\Big|u|_{I_j}\in H^k(I_j),\ \forall I_j\in\mathcal{I}_h \text{ and } \sum_{I_j\in\mathcal{I}_h}||u||^2_{k,I_j}<\infty\Big\}, \tag{3.2}$$

with norms:

$$||u||_{k,\mathcal{T}_h}=\Big(\sum_{K\in\mathcal{T}_h}||u||^2_{k,K}\Big)^{\frac{1}{2}},\qquad ||u||_{k,\mathcal{I}_h}=\Big(\sum_{I_j\in\mathcal{I}_h}||u||^2_{k,I_j}\Big)^{\frac{1}{2}}. \tag{3.3}$$

Further, we define

$$L^2(\mathcal{I}_h,H^k(\mathcal{T}_h))=\Big\{u\Big|u(\cdot,t)\in H^k(\mathcal{T}_h),\forall t\in I, \text{ and}\int_{I_j}\|u(\cdot,t)\|^2_{k,\mathcal{T}_h}\mathrm{d}t<\infty,\forall I_j\in\mathcal{I}_h\Big\}, \tag{3.4}$$

with norm

$$|||u|||_{h,k,0}=\Big(\sum_{I_j\in\mathcal{I}_h}\int_{I_j}\|u(\cdot,t)\|^2_{k,\mathcal{T}_h}\mathrm{d}t\Big)^{\frac{1}{2}}; \tag{3.5}$$

and

$$H^k(\mathcal{I}_h,L^2(\mathcal{T}_h))=\Big\{u\Big|u(\mathbf{x},\cdot)\in H^k(\mathcal{I}_h),\forall\mathbf{x}\in\Omega, \text{ and}\int_K\|u(\mathbf{x},\cdot)\|^2_{k,\mathcal{I}_h}\mathrm{d}\mathbf{x}<\infty,\forall K\in\mathcal{T}_h\Big\}, \tag{3.6}$$

with norm

$$|||u|||_{h,0,k}=\Big(\sum_{K\in\mathcal{T}_h}\int_K\|u(\mathbf{x},\cdot)\|^2_{k,\mathcal{I}_h}\mathrm{d}\mathbf{x}\Big)^{\frac{1}{2}}. \tag{3.7}$$

We shall use $|||\cdot|||_h$ as an abbreviation of $|||\cdot|||_{h,0,0}$. Corresponding vector functional spaces are denoted by $\big(H^k(\mathcal{T}_h)\big)^3$, $\big(L^2(\mathcal{I}_h,H^k(\mathcal{T}_h))\big)^3$ and $\big(H^k(\mathcal{I}_h,L^2(\mathcal{T}_h))\big)^3$, respectively. For $\mathbf{U}=(\mathbf{H},\mathbf{E})^T$, define

$$\|\mathbf{U}\|=\big(\|\mathbf{H}\|^2+\|\mathbf{E}\|^2\big)^{1/2}, \tag{3.8}$$

and

$$\|\mathbf{Q}^{1/2}\mathbf{U}\|=\big(\mu\|\mathbf{H}\|^2+\epsilon\|\mathbf{E}\|^2\big)^{1/2}, \tag{3.9}$$

where $||\cdot||$ stands for any norm introduced above.

3.1 L^2-stability

According to (2.14), we define bilinear forms,

$$\begin{aligned}B_{I_j,K}(\mathbf{U}_h,\mathbf{v}_h)=&-\int_{I_j}\int_K\mathbf{Q}\mathbf{U}_h\cdot\frac{\partial\mathbf{v}_h}{\partial t}\mathrm{d}\mathbf{x}\mathrm{d}t+\lambda\int_{I_j}\int_K\mathbf{Q}\mathbf{U}_h\cdot\mathbf{v}_h\mathrm{d}\mathbf{x}\mathrm{d}t\\&+\int_{I_j}\sum_{e\in\partial K}\int_e(\widehat{\mathbf{f}(\mathbf{U}_h)\cdot\mathbf{n}_K})\cdot\mathbf{v}_h\mathrm{d}s\mathrm{d}t-\int_{I_j}\int_K\mathbf{f}(\mathbf{U}_h)\cdot\nabla\mathbf{v}_h\mathrm{d}\mathbf{x}\mathrm{d}t\end{aligned}$$

$$+\int_{I_j}\int_K \tilde{\mathbf{G}}(\mathbf{U}_h)\cdot\mathbf{v}_h\mathrm{d}\mathbf{x}\mathrm{d}t+\int_K(\mathbf{Q}\hat{\mathbf{U}}_h\cdot\mathbf{v}_h)|_{t_j}^{t_{j+1}}\mathrm{d}\mathbf{x}, \tag{3.10}$$

and

$$\mathbf{B}_h(\mathbf{U}_h,\mathbf{v}_h)=\sum_{j=0}^{n-1}\sum_{K\in\mathcal{T}_h}\mathbf{B}_{I_j,K}(\mathbf{U}_h,\mathbf{v}_h). \tag{3.11}$$

Thus (2.14) implies that the numerical solution $\mathbf{U}_h$ satisfies

$$\mathbf{B}_h(\mathbf{U}_h,\mathbf{v}_h)=0,\quad \forall\mathbf{v}_h\in\mathbf{V}_h^{r,k} \tag{3.12}$$

Then, we have the following L^2-stability for our space-time DG scheme, i.e.,

Proposition 3.1 Assume that $\tilde{\kappa}(t)\in L^\infty([0,T])$ and $\mathbf{U}_h=(\mathbf{H}_h^\lambda,\mathbf{E}_h^\lambda)^T$ is the solution of (2.14). Then,

$$\mu||\mathbf{H}_h^\lambda(\mathbf{x},T^-)||_{0,\mathcal{T}_h}^2+\epsilon||\mathbf{E}_h^\lambda(\mathbf{x},T^-)||_{0,\mathcal{T}_h}^2+\Theta_{T,\mathcal{T}_h}(\mathbf{U}_h)\le\mu||\mathbf{H}_0||_{0,\mathcal{T}_h}^2+\epsilon||\mathbf{E}_0||_{0,\mathcal{T}_h}^2,$$

where

$$\begin{aligned}\Theta_{T,\mathcal{T}_h}(\mathbf{U}_h)=&\int_0^T\sum_{e\subset\mathcal{E}_\mathcal{I}}\int_e\left(Z|[\![\mathbf{H}_h^\lambda]\!]_T|^2+\frac{1}{Z}|[\![\mathbf{E}_h^\lambda]\!]_T|^2\right)\mathrm{d}s\mathrm{d}t\\&+2\int_0^T\sum_{e\subset\mathcal{E}_\mathcal{D}}\int_e\frac{1}{Z}|\mathbf{n}\times(\mathbf{E}_h^\lambda)^{\mathrm{int}}|^2\mathrm{d}s\mathrm{d}t.\end{aligned}$$

Proof Let $\mathbf{v}_h=\mathbf{U}_h$ in (3.11) we have

$$\begin{aligned}&\mathbf{B}_h(\mathbf{U}_h,\mathbf{U}_h)\\=&-\sum_{j=0}^{n-1}\sum_{K\in\mathcal{T}_h}\int_{I_j}\int_K\mathbf{Q}\mathbf{U}_h\cdot\frac{\partial\mathbf{U}_h}{\partial t}\mathrm{d}\mathbf{x}\mathrm{d}t+\lambda\sum_{j=0}^{n-1}\sum_{K\in\mathcal{T}_h}\int_{I_j}\int_K\mathbf{Q}\mathbf{U}_h\cdot\mathbf{U}_h\mathrm{d}\mathbf{x}\mathrm{d}t\\&+\sum_{j=0}^{n-1}\sum_{K\in\mathcal{T}_h}\int_{I_j}\int_{\partial K}\left(\mathbf{f}(\widehat{\mathbf{U}_h)\cdot\mathbf{n}_K}\right)\cdot\mathbf{U}_h\mathrm{d}s\mathrm{d}t-\sum_{j=0}^{n-1}\sum_{K\in\mathcal{T}_h}\int_{I_j}\int_K\mathbf{f}(\mathbf{U}_h)\cdot\nabla\mathbf{U}_h\mathrm{d}\mathbf{x}\mathrm{d}t\\&+\sum_{j=0}^{n-1}\sum_{K\in\mathcal{T}_h}\int_{I_j}\int_K\tilde{\mathbf{G}}(\mathbf{U}_h)\cdot\mathbf{U}_h\mathrm{d}\mathbf{x}\mathrm{d}t+\sum_{j=0}^{n-1}\int_\Omega(\mathbf{Q}\hat{\mathbf{U}}_h\cdot\mathbf{U}_h)|_{t_j}^{t_{j+1}}\mathrm{d}\mathbf{x}.\end{aligned} \tag{3.13}$$

Following the proof of Proposition 3.1 in [29], we have

$$\begin{aligned}&-\sum_{j=0}^{n-1}\sum_{K\in\mathcal{T}_h}\int_{I_j}\int_K\mathbf{Q}\mathbf{U}_h\cdot\frac{\partial\mathbf{U}_h}{\partial t}\mathrm{d}\mathbf{x}\mathrm{d}t+\sum_{j=0}^{n-1}\sum_{K\in\mathcal{T}_h}\int_K\left(\mathbf{Q}\hat{\mathbf{U}}_h\cdot\mathbf{U}_h\right)|_{t_j}^{t_{j+1}}\mathrm{d}\mathbf{x}\\\ge&\frac{1}{2}||\mathbf{Q}^{1/2}\mathbf{U}_h(\cdot,T^-)||_{0,\mathcal{T}_h}^2-\frac{1}{2}||\mathbf{Q}^{1/2}\mathbf{U}_0||_{0,\mathcal{T}_h}^2.\end{aligned} \tag{3.14}$$

According to the proof of Lemma 3.1 in [28], we have the identity

$$\sum_{j=0}^{n-1}\sum_{K\in\mathcal{T}_h}\left(\int_{I_j}\int_{\partial K}\left(\mathbf{f}(\widehat{\mathbf{U}_h)\cdot\mathbf{n}_K}\right)\cdot\mathbf{U}_h\mathrm{d}s\mathrm{d}t-\int_{I_j}\int_K\mathbf{f}(\mathbf{U}_h)\cdot\nabla\mathbf{U}_h\mathrm{d}\mathbf{x}\mathrm{d}t\right)=\frac{1}{2}\Theta_{T,\mathcal{T}_h}(\mathbf{U}_h). \tag{3.15}$$

Then, the rest work is to handle the integral term. By using the definition of $\tilde{\mathbf{G}}$ and $\mathbf{G}$ in (2.10), we have

$$\int_I\int_\Omega\tilde{\mathbf{G}}(\mathbf{U}_h)\cdot\mathbf{U}_h\mathrm{d}\mathbf{x}\mathrm{d}t=c|||\mathbf{E}_h^\lambda|||_h^2+\sum_{j=0}^{n-1}\int_{I_j}\int_\Omega\int_0^t\kappa(t-s)\mathbf{E}_h^\lambda(\mathbf{x},s)\mathrm{d}s\cdot\mathbf{E}_h^\lambda(\mathbf{x},t)\mathrm{d}\mathbf{x}\mathrm{d}t. \tag{3.16}$$

According to the definition of $\kappa(t)$, we have $|\kappa(t)| \leq |\tilde{\kappa}(t)|$. Since $\tilde{\kappa}(t) \in L^\infty([0,T])$, direct calculation leads to

$$\left|\sum_{j=0}^{n-1}\sum_{K\in\mathcal{T}_h}\int_{I_j}\int_K\int_0^t \kappa(t-s)\mathbf{E}_h^\lambda(\mathbf{x},s)\mathrm{d}s\cdot\mathbf{E}_h^\lambda(\mathbf{x},t)\mathrm{d}\mathbf{x}\mathrm{d}t\right| \leq ||\tilde{\kappa}||_\infty T|||\mathbf{E}_h^\lambda|||_h^2. \tag{3.17}$$

In fact

$$\begin{aligned}
&\left|\sum_{j=0}^{n-1}\sum_{K\in\mathcal{T}_h}\int_{I_j}\int_K\int_0^t \kappa(t-s)\mathbf{E}_h^\lambda(\mathbf{x},s)\mathrm{d}s\cdot\mathbf{E}_h^\lambda(\mathbf{x},t)\mathrm{d}\mathbf{x}\mathrm{d}t\right| \\
\leq&\sum_{j=0}^{n-1}\int_{I_j}\sum_{K\in\mathcal{T}_h}\int_K\int_0^t |\kappa(t-s)||\mathbf{E}_h^\lambda(\mathbf{x},s)||\mathbf{E}_h^\lambda(\mathbf{x},t)|\mathrm{d}s\mathrm{d}\mathbf{x}\mathrm{d}t \\
\leq&\frac{||\kappa||_\infty}{2}\sum_{j=0}^{n-1}\int_{I_j}\int_0^{t_{j+1}}(||\mathbf{E}_h^\lambda(\cdot,s)||_{0,\mathcal{T}_h}^2+||\mathbf{E}_h^\lambda(\cdot,t)||_{0,\mathcal{T}_h}^2)\mathrm{d}s\mathrm{d}t \\
\leq&\frac{||\tilde{\kappa}||_\infty}{2}\left(n\tau\sum_{j=0}^{n-1}\int_{I_j}||\mathbf{E}_h^\lambda(\cdot,t)||_{0,\mathcal{T}_h}^2\mathrm{d}t+T\sum_{j=0}^{n-1}\int_{I_j}||\mathbf{E}_h^\lambda(\cdot,t)||_{0,\mathcal{T}_h}^2\mathrm{d}t\right) \\
\leq&||\tilde{\kappa}||_\infty T|||\mathbf{E}_h^\lambda|||_h^2,
\end{aligned}$$

where the fact $n\tau = T$ is used.

Substituting (3.14), (3.15), (3.16) and (3.17) into (3.13), and then using the equation (3.12), we obtain

$$\begin{aligned}
&\frac{1}{2}||\mathbf{Q}^{1/2}\mathbf{U}_h(\cdot,T^-)||_{0,\mathcal{T}_h}^2+\lambda|||\mathbf{Q}^{1/2}\mathbf{U}_h|||_h^2+\frac{1}{2}\Theta_{T,\mathcal{T}_h}(\mathbf{U}_h)+c|||\mathbf{E}_h^\lambda|||_h^2 \\
\leq&\frac{1}{2}\big(\mu||\mathbf{H}_0||_{0,\mathcal{T}_h}^2+\epsilon||\mathbf{E}_0||_{0,\mathcal{T}_h}^2\big)+\left|\int_0^T\int_\Omega\int_0^t \kappa(t-s)\mathbf{E}_h^\lambda(\mathbf{x},s)\mathrm{d}s\cdot\mathbf{E}_h^\lambda(\mathbf{x},t)\mathrm{d}\mathbf{x}\mathrm{d}t\right| \\
\leq&\frac{1}{2}\big(\mu||\mathbf{H}_0||_{0,\mathcal{T}_h}^2+\epsilon||\mathbf{E}_0||_{0,\mathcal{T}_h}^2\big)+||\tilde{\kappa}||_\infty T|||\mathbf{E}_h^\lambda|||_h^2
\end{aligned}$$

By choosing $\lambda > \frac{||\tilde{\kappa}||_\infty T}{\epsilon}$, we can eliminate the integral term from the right hand side of the equation. Thus the conclusion can be obtained by using the fact that c is a nonnegative constant.

□

3.2 Error estimates

Now, we turn to the error estimates of the space-time DG solution. For this purpose, we introduce two element-wise projection operators $\mathbf{\Pi}_h$ and $\mathbb{P}_h$ and their corresponding approximation results which will be used in the proof of the L^2 error estimates later. First we introduce a projection operator $\mathbf{\Pi}_h : H^{r+1}(\mathcal{I}_h) \to S_{h,I}^r$ such that

$$\mathbf{\Pi}_h u(t_{j+1}^-) = u(t_{j+1}^-), \tag{3.18}$$

$$\int_{I_j}(u-\mathbf{\Pi}_h u)\,v\mathrm{d}t = 0, \quad \forall v\in P_{r-1}(I_j), \quad j=0,1,\cdots,n-1, \quad r\geq 1. \tag{3.19}$$

Furthermore, we have the following error estimate [4].

Lemma 3.2 For any $u \in H^{r+1}(I_j)$, we have

$$||u-\mathbf{\Pi}_h u||_{0,I_j} \leq C\tau^{r+1}||u||_{I_j,r+1}. \tag{3.20}$$

Moreover, we also need the element-wise L^2-projection operator $\mathbb{P}_h : H^{k+1}(\mathcal{T}_h) \to S^k_{h,\Omega}$, such that

$$\int_K \mathbb{P}_h uv \mathrm{d}\mathbf{x} = \int_K uv \mathrm{d}\mathbf{x}, \quad \forall v \in P^k(K), \quad \forall K \in \mathcal{T}_h. \tag{3.21}$$

For this L^2 projection operator, we have the following approximation lemma.

Lemma 3.3 ([9]) Let $u \in H^{k+1}(K)$, and $\mathbb{P}_h u$ its L^2-projection into $P^k(K)$. Then

$$||u - \mathbb{P}_h u||_{0,K} \le Ch^{k+1}|u|_{k+1,K},$$

$$||u - \mathbb{P}_h u||_{0,\partial K} \le Ch^{k+1/2}|u|_{k+1,K}.$$

The error analysis of time-dependent problems is often more difficult than that for the time-independent ones. Actually, the main difficulty is how to decompose the error into the temporal part and spatial part which can be handled independently. In our work we introduce an operator decomposition as follow [6, 10]:

$$I - \mathbf{\Pi}_h \otimes \mathbb{P}_h = (I - \mathbf{\Pi}_h) + (I - \mathbb{P}_h) - (I - \mathbf{\Pi}_h) \otimes (I - \mathbb{P}_h), \tag{3.22}$$

which will be used to decompose the error. In terms of the orthogonality relations in (3.19) and (3.21), we have

$$\int_{I_j} \left[(I - \mathbf{\Pi}_h) \otimes (I - \mathbb{P}_h)u\right] v = 0, \quad \forall v \in P^{r-1}(I_j), \quad j = 0, 1, \cdots, n-1, \quad r \ge 1 \tag{3.23}$$

$$\int_K \left[(I - \mathbf{\Pi}_h) \otimes (I - \mathbb{P}_h)u\right] v = 0, \quad \forall v \in P^k(K), \quad K \in \mathcal{T}_h \tag{3.24}$$

Actually (3.23) can be obtained by a straightforward implementation of (3.19). On the other hand, (3.24) can be obtained immediately considering the fact that $I - \Pi_h$ and $I - \mathbb{P}_h$ are independent of each other.

It is noted that the numerical fluxes defined in (2.15), (2.16) and (2.17) are consistent except for $\widehat{\mathbf{U}_h(0)} = \mathbb{P}_h \mathbf{U}_0$. Consequently, according to (2.13) and (2.14), we have

$$\mathbf{B}_{I_j,K}(\mathbf{e}, \mathbf{v}_h) = 0, \quad j = 1, 2, \cdots, n-1, \tag{3.25}$$

where $\mathbf{e} = \mathbf{U} - \mathbf{U}_h$. On behalf of the definition of the numerical fluxes and the projection operator $\mathbb{P}_h$, we have

$$\begin{aligned} &- \int_{I_0}\int_K \mathbf{Q}\mathbf{e} \cdot (\mathbf{v}_h)_t \mathrm{d}\mathbf{x}\mathrm{d}t + \lambda \int_{I_0}\int_K \mathbf{Q}\mathbf{e} \cdot \mathbf{v}_h \mathrm{d}\mathbf{x}\mathrm{d}t + \int_{I_j}\int_{\partial K} (\widehat{\mathbf{f}(\mathbf{e}) \cdot \mathbf{n}}_K) \cdot \mathbf{v}_h \mathrm{d}s\mathrm{d}t \\ &- \int_{I_0}\int_K f(\mathbf{e}) \cdot \nabla \mathbf{v}_h \mathrm{d}\mathbf{x}\mathrm{d}t + \int_{I_j}\int_K \tilde{\mathbf{G}}(\mathbf{e}, t) \cdot \mathbf{v}_h(\mathbf{x}, t) \mathrm{d}\mathbf{x}\mathrm{d}t + \int_K \mathbf{Q}\mathbf{e}(\mathbf{x}, t_1^-) \cdot \mathbf{v}_h(\mathbf{x}, t_1^-) \mathrm{d}\mathbf{x} \\ &= 0. \end{aligned} \tag{3.26}$$

Denote the left-hand side of (3.26) by $\bar{\mathbf{B}}_{I_0,K}(\mathbf{e}, \mathbf{v}_h)$. Then by (3.25) and (3.26), we obtain the error equation

$$\bar{\mathbf{B}}_h(\mathbf{e}, \mathbf{v}_h) = 0, \quad \mathbf{v}_h \in \mathbf{V}_h^{r,k}, \tag{3.27}$$

where

$$\bar{\mathbf{B}}_h(\mathbf{e}, \mathbf{v}_h) = \sum_{j=1}^{n-1} \sum_{K \in \mathcal{T}_h} B_{I_j,K}(\mathbf{e}, \mathbf{v}_h) + \sum_{K \in \mathcal{T}_h} \bar{\mathbf{B}}_{I_0,K}(\mathbf{e}, \mathbf{v}_h). \tag{3.28}$$

The error $\mathbf{e}$ can be decomposed into

$$\mathbf{e} = \mathbf{U} - \mathbf{\Pi}_h \otimes \mathbb{P}_h \mathbf{U} - (\mathbf{U}_h - \mathbf{\Pi}_h \otimes \mathbb{P}_h \mathbf{U}) = \mathbf{R} - \theta. \tag{3.29}$$

where

$$\mathbf{R} = \mathbf{U} - \mathbf{\Pi}_h \otimes \mathbb{P}_h \mathbf{U}, \quad \theta = \mathbf{U}_h - \mathbf{\Pi}_h \otimes \mathbb{P}_h \mathbf{U}.$$

Substituting $\mathbf{e} = \mathbf{R} - \theta$ into (3.27), we get

$$\bar{\mathbf{B}}_h(\mathbf{R}, \mathbf{v}_h) = \bar{\mathbf{B}}_h(\theta, \mathbf{v}_h), \quad \forall \mathbf{v}_h \in \mathbf{V}_h^{r,k}. \tag{3.30}$$

Obviously, $\theta \in \mathbf{V}_h^{r,k}$, then setting $\mathbf{v}_h = \theta$ in (3.30) leads to

$$\bar{\mathbf{B}}_h(\mathbf{R}, \theta) = \bar{\mathbf{B}}_h(\theta, \theta). \tag{3.31}$$

Noting that $\mathbf{e}$, $\mathbf{R}$ and θ have their corresponding $\mathbf{H}$ and $\mathbf{E}$ parts, we shall use the following notations:

$$\mathbf{e} = \begin{pmatrix} \mathbf{e}_1 \\ \mathbf{e}_2 \end{pmatrix}, \quad \mathbf{R} = \begin{pmatrix} \mathbf{R}_1 \\ \mathbf{R}_2 \end{pmatrix}, \quad \theta = \begin{pmatrix} \theta_1 \\ \theta_2 \end{pmatrix},$$

where index 1, 2 indicates $\mathbf{H}$ and $\mathbf{E}$ parts, respectively.

Lemma 3.4 In terms of $\bar{\mathbf{B}}_h(\theta, \theta)$, we have the following estimate

$$\begin{aligned} \bar{\mathbf{B}}_h(\theta, \theta) \geq & \frac{1}{2}||\mathbf{Q}^{1/2}\theta(\cdot, T^-)||^2_{0,\mathcal{T}_h} + \frac{1}{2}||\mathbf{Q}^{1/2}\theta(\cdot, 0^+)||^2_{0,\mathcal{T}_h} + \lambda|||\mathbf{Q}^{1/2}\theta|||^2_h + \frac{1}{2}\Theta_{T,\mathcal{T}_h}(\theta) \\ & + c|||\theta_2|||^2_h + \sum_{j=0}^{n-1} \sum_{K \in \mathcal{T}_h} \int_{I_j} \int_K \int_0^t \kappa(t-s)\theta_2(\mathbf{x}, s)\mathrm{d}s \cdot \theta_2(\mathbf{x}, t)\mathrm{d}\mathbf{x}\mathrm{d}t \end{aligned} \tag{3.32}$$

The proof of this lemma can be done by following the proof of Lemma 3.3 in [29].

Now we turn to the estimate of $\bar{\mathbf{B}}_h(\mathbf{R}, \theta)$. In terms of (3.10), (3.26) and (3.28), we have

$$\begin{aligned} \bar{B}_h(\mathbf{R}, \theta) = & -\sum_{j=0}^{n-1} \sum_{K \in \mathcal{T}_h} \int_{I_j} \int_K (\mathbf{Q}\mathbf{R} \cdot \theta_t + \lambda \mathbf{Q}\mathbf{R} \cdot \theta + c\mathbf{R}_2 \cdot \theta_2)\mathrm{d}\mathbf{x}\mathrm{d}t \\ & + \sum_{j=0}^{n-1} \sum_{K \in \mathcal{T}_h} \left(\int_{I_j} \int_{\partial K} \left(\widehat{\mathbf{f}(\mathbf{R}) \cdot \mathbf{n}_K} \right) \cdot \theta \mathrm{d}\mathbf{x}\mathrm{d}t - \int_{I_j} \int_K \mathbf{f}(\mathbf{R}) \cdot \nabla\theta \mathrm{d}\mathbf{x}\mathrm{d}t \right) \\ & + \sum_{j=0}^{n-1} \sum_{K \in \mathcal{T}_h} \int_{I_j} \int_K \left(\int_0^t \kappa(t-s)\mathbf{R}_2(\mathbf{x}, s)\mathrm{d}s \right) \cdot \theta_2(\mathbf{x}, t)\mathrm{d}\mathbf{x}\mathrm{d}t \\ & + \sum_{j=1}^{n-1} \sum_{K \in \mathcal{T}_h} \int_K \left(\mathbf{Q}\hat{\mathbf{R}} \cdot \theta \right) |_{t_j}^{t_{j+1}} \mathrm{d}\mathbf{x} + \sum_{K \in \mathcal{T}_h} \int_K \mathbf{Q}\mathbf{R}(\mathbf{x}, t_1^-) \cdot \theta(\mathbf{x}, t_1^-)\mathrm{d}\mathbf{x}. \end{aligned} \tag{3.33}$$

By using the operator decomposition introduced in (3.22), $\mathbf{R}$ can be decomposed into three parts, i.e.,

$$\mathbf{R} = (I - \mathbf{\Pi}_h \otimes \mathbb{P}_h)\mathbf{U} = (I - \mathbf{\Pi}_h)\mathbf{U} + (I - \mathbb{P}_h)\mathbf{U} - (I - \mathbf{\Pi}_h) \otimes (I - \mathbb{P}_h)\mathbf{U}. \tag{3.34}$$

Denoted by

$$\xi = (I - \mathbf{\Pi}_h)\mathbf{U}, \quad \eta = (I - \mathbb{P}_h)\mathbf{U}, \quad \rho = -(I - \mathbf{\Pi}_h) \otimes (I - \mathbb{P}_h)\mathbf{U},$$

then

$$\mathbf{R} = \xi + \eta + \rho. \tag{3.35}$$

According to the properties of projection Π_h, i.e., (3.18), we have

$$\xi(\mathbf{x}, t_j^-) = 0, \qquad \rho(\mathbf{x}, t_j^-) = 0, \quad \forall \mathbf{x} \in \Omega, \quad j = 1, 2, \cdots, n. \tag{3.36}$$

Due to $\theta, \theta_t \in \mathbf{V}_h^{r,k}$, thus $\theta_1(\mathbf{x}, \cdot)|_K$, $(\theta_1)_t(\mathbf{x}, \cdot)|_K$, $\theta_2(\mathbf{x}, \cdot)|_K$, $(\theta_2)_t(\mathbf{x}, \cdot)|_K \in (\mathbf{P}^k(K))^3$, $(\theta_1)_t(\cdot, t)|_{I_j}$, $(\theta_2)_t(\cdot, t)|_{I_j} \in (P^{r-1}(I_j))^3$. According to the definition of the two projection operators $\mathbf{\Pi}_h$ and $\mathbb{P}_h$ and (3.23) and (3.24), we have the following orthogonality relations, i.e.,

$$\int_{I_j} \xi(\mathbf{x}, t) \cdot \theta_t(\mathbf{x}, t) \mathrm{d}t = 0, \qquad \int_{I_j} \rho(\mathbf{x}, t) \cdot \theta_t(\mathbf{x}, t) \mathrm{d}t = 0, \quad \forall \mathbf{x} \in \Omega, \tag{3.37}$$

$$\int_K \eta(\mathbf{x}, t) \cdot \theta_t(\mathbf{x}, t) \mathrm{d}\mathbf{x} = 0, \qquad \int_K \rho(\mathbf{x}, t) \cdot \theta_t(\mathbf{x}, t) \mathrm{d}\mathbf{x} = 0, \quad \forall t \in (0, T], \tag{3.38}$$

$$\int_K \eta(\mathbf{x}, t) \cdot \theta(\mathbf{x}, t) \mathrm{d}\mathbf{x} = 0, \qquad \int_K \rho(\mathbf{x}, t) \cdot \theta(\mathbf{x}, t) \mathrm{d}\mathbf{x} = 0, \quad \forall t \in (0, T]. \tag{3.39}$$

As a consequence,

$$\int_{I_j} \int_K \mathbf{QR} \cdot \theta_t \mathrm{d}\mathbf{x}\mathrm{d}t = \int_{I_j} \int_K \mathbf{Q}(\xi + \eta + \rho) \cdot \theta_t \mathrm{d}\mathbf{x}\mathrm{d}t = 0, \quad j = 0, 1, \cdots, n-1, K \in \mathcal{T}_h. \tag{3.40}$$

On the other hand,

$$\begin{aligned}
\int_K \left(\mathbf{Q}\hat{\mathbf{R}} \cdot \theta \right) |_{t_j}^{t_{j+1}} \mathrm{d}\mathbf{x} &= \int_K \mathbf{Q} \left(\mathbf{R}(\mathbf{x}, t_{j+1}^-) \cdot \theta(\mathbf{x}, t_{j+1}^-) - \mathbf{R}(\mathbf{x}, t_j^-) \cdot \theta(\mathbf{x}, t_j^+) \right) \mathrm{d}\mathbf{x} \\
&= \int_K \mathbf{Q} \left(\xi(\mathbf{x}, t_{j+1}^-) + \eta(\mathbf{x}, t_{j+1}^-) + \rho(\mathbf{x}, t_{j+1}^-) \right) \cdot \theta(\mathbf{x}, t_{j+1}^-) \mathrm{d}\mathbf{x} \\
&\quad - \int_K \mathbf{Q} \left(\xi(\mathbf{x}, t_j^-) + \eta(\mathbf{x}, t_j^-) + \rho(\mathbf{x}, t_j^-) \right) \cdot \theta(\mathbf{x}, t_j^+) \mathrm{d}\mathbf{x} \\
&= 0, \qquad j = 1, \cdots, n-1.
\end{aligned} \tag{3.41}$$

Furthermore,

$$\int_K \mathbf{QR}(\mathbf{x}, t_1^-) \cdot \theta(\mathbf{x}, t_1^-) \mathrm{d}\mathbf{x} = \int_K \mathbf{Q} \left(\xi(\mathbf{x}, t_1^-) + \eta(\mathbf{x}, t_1^-) + \rho(\mathbf{x}, t_1^-) \right) \cdot \theta(\mathbf{x}, t_1^-) \mathrm{d}\mathbf{x} = 0. \tag{3.42}$$

Implementing (3.40), (3.41) and (3.42) in (3.33), we have

$$\begin{aligned}
\bar{B}_h(\mathbf{R}, \theta) &= \sum_{j=0}^{n-1} \sum_{K \in \mathcal{T}_h} \int_{I_j} \int_K \left(\lambda \mathbf{QR} \cdot \theta + c \mathbf{R}_2 \cdot \theta_2 \right) \mathrm{d}\mathbf{x}\mathrm{d}t \\
&\quad + \sum_{j=0}^{n-1} \sum_{K \in \mathcal{T}_h} \int_{I_j} \left(\int_{\partial K} \left(\widehat{\mathbf{f}(\mathbf{R}) \cdot \mathbf{n}}_K \right) \cdot \theta \mathrm{d}\mathbf{x} - \int_K \mathbf{f}(\mathbf{R}) \cdot \nabla \theta \mathrm{d}\mathbf{x} \right) \mathrm{d}t \\
&\quad + \sum_{j=0}^{n-1} \sum_{K \in \mathcal{T}_h} \int_{I_j} \int_K \left(\int_0^t \kappa(t-s) \mathbf{R}_2(\mathbf{x}, s) \mathrm{d}s \right) \cdot \theta_2(\mathbf{x}, t) \mathrm{d}\mathbf{x}\mathrm{d}t.
\end{aligned} \tag{3.43}$$

Lemma 3.5 In terms of $\bar{\mathbf{B}}_h(\mathbf{R}, \theta)$, we have

$$\begin{aligned}
\bar{\mathbf{B}}_h(\mathbf{R}, \theta) &\le C h^{2k+1} |||\mathbf{U}|||_{h,k+1,0}^2 + C\tau^{2r+2} |||\mathbf{U}|||_{h,0,r+1}^2 \\
&\quad + C\tau^{2r+2} \left(|||\nabla \times \mathbf{H}^\lambda|||_{h,0,r+1}^2 + |||\nabla \times \mathbf{E}^\lambda|||_{h,0,r+1}^2 \right) + \frac{1}{2} \Theta_{T, \mathcal{T}_h}(\theta) \\
&\quad + \frac{1+\lambda}{2} |||\mathbf{Q}^{1/2} \theta|||_h^2 + \left(c + \frac{T\epsilon ||\tilde{\kappa}||_\infty}{2} \right) |||\theta_2|||_h^2 + C\tau^{2r+2} T |||\mathbf{E}^\lambda|||_{h,0,r+1}^2.
\end{aligned} \tag{3.44}$$

Proof In (3.43), set

$$\mathcal{A}_1^j = \sum_{K\in\mathcal{T}_h}\int_{I_j}\int_K (\lambda\mathbf{Q}\mathbf{R}\cdot\theta + c\mathbf{R}_2\cdot\theta_2)\,\mathrm{d}\mathbf{x}\mathrm{d}t, \tag{3.45}$$

$$\mathcal{A}_2^j = \sum_{K\in\mathcal{T}_h}\int_{I_j}\left(\int_{\partial K}\left(\widehat{\mathbf{f}(\mathbf{R})\cdot\mathbf{n}_K}\right)\cdot\theta\mathrm{d}\mathbf{x} - \int_K \mathbf{f}(\mathbf{R})\cdot\nabla\theta\mathrm{d}\mathbf{x}\right)\mathrm{d}t, \tag{3.46}$$

$$\mathcal{A}_3^j = \sum_{K\in\mathcal{T}_h}\int_{I_j}\int_K\left(\int_0^t \kappa(t-s)\mathbf{R}_2(\mathbf{x},s)\mathrm{d}s\right)\cdot\theta_2(\mathbf{x},t)\mathrm{d}\mathbf{x}\mathrm{d}t. \tag{3.47}$$

In order to estimate $\bar{\mathbf{B}}_h(\mathbf{R},\theta)$, we need to estimate $\mathcal{A}_1^j$, $\mathcal{A}_2^j$ and $\mathcal{A}_3^j$.

Following the same strategy in the proof of Lemma 3.4 in [29], we have

$$\mathcal{A}_1^j \le \lambda C\tau^{2r+2}\sum_{K\in\mathcal{T}_h}\int_K ||\mathbf{U}(\mathbf{x},\cdot)||^2_{r+1,I_j}\mathrm{d}\mathbf{x} + \int_{I_j}\left(\frac{\lambda}{2}||\mathbf{Q}^{1/2}\theta(\cdot,t)||^2_{0,\mathcal{T}_h} + c||\theta_2(\cdot,t)||^2_{0,\mathcal{T}_h}\right)\mathrm{d}t, \tag{3.48}$$

and

$$\begin{aligned}\mathcal{A}_2^j \le{}& C\tau^{2r+2}\sum_{K\in\mathcal{T}_h}\int_K\left(||\nabla\times\mathbf{H}^\lambda(\mathbf{x},\cdot)||^2_{r+1,I_j} + ||\nabla\times\mathbf{E}^\lambda(\mathbf{x},\cdot)||^2_{r+1,I_j}\right)\mathrm{d}\mathbf{x}\\ &+Ch^{2k+1}\int_{I_j}||\mathbf{U}(\cdot,t)||^2_{k+1,\mathcal{T}_h}\mathrm{d}t + \frac{1}{2}\int_{I_j}||\mathbf{Q}^{1/2}\theta||^2_{0,\mathcal{T}_h}\mathrm{d}t\\ &+\frac{1}{2}\int_{I_j}\sum_{e\subset\mathcal{E}_\mathcal{I}}\int_e\left(Z|[\![\theta_1]\!]_T|^2 + \frac{1}{Z}|[\![\theta_2]\!]_T|^2\right)\mathrm{d}s\mathrm{d}t + \frac{1}{Z}\int_{I_j}\sum_{e\subset\mathcal{E}_\mathcal{D}}\int_e|\mathbf{n}\times\theta_2^{\mathrm{int}}|^2\mathrm{d}s\mathrm{d}t,\end{aligned} \tag{3.49}$$

Thus, we only need to estimate the integral term $\mathcal{A}_3^j$ here. By using the orthogonal properties (3.37) and the Young's inequality, we obtain

$$\begin{aligned}\mathcal{A}_3^j &= \sum_{K\in\mathcal{T}_h}\int_{I_j}\int_K\int_0^t\kappa(t-s)\mathbf{R}_2(\mathbf{x},s)\mathrm{d}s\cdot\theta_2(\mathbf{x},t)\mathrm{d}\mathbf{x}\mathrm{d}t\\ &= \sum_{K\in\mathcal{T}_h}\int_{I_j}\int_0^t\kappa(t-s)\int_K(\xi_2(\mathbf{x},s)+\eta_2(\mathbf{x},s)+\rho_2(\mathbf{x},s))\cdot\theta_2(\mathbf{x},t)\mathrm{d}\mathbf{x}\mathrm{d}s\mathrm{d}t\\ &= \sum_{K\in\mathcal{T}_h}\int_K\int_{I_j}\int_0^t\kappa(t-s)\xi_2(\mathbf{x},s)\cdot\theta_2(\mathbf{x},t)\mathrm{d}\mathbf{x}\mathrm{d}s\mathrm{d}t\\ &\le ||\tilde{\kappa}||_\infty\sum_{K\in\mathcal{T}_h}\int_K\int_{I_j}\int_0^t\left(\frac{1}{2\epsilon}|\xi_2(\mathbf{x},s)|^2 + \frac{\epsilon}{2}|\theta_2(\mathbf{x},t)|^2\right)\mathrm{d}s\mathrm{d}t\mathrm{d}\mathbf{x}.\end{aligned} \tag{3.50}$$

Moreover, careful calculations lead to

$$\begin{aligned}&\sum_{K\in\mathcal{T}_h}\int_K\int_{I_j}\int_0^t\left(\frac{1}{2\epsilon}|\xi_2(\mathbf{x},s)|^2 + \frac{\epsilon}{2}|\theta_2(\mathbf{x},t)|^2\right)\mathrm{d}s\mathrm{d}t\mathrm{d}\mathbf{x}\\ \le{}& \sum_{K\in\mathcal{T}_h}\int_K\int_{I_j}\sum_{i=0}^j\int_{I_i}\left(\frac{1}{2\epsilon}|\xi_2(\mathbf{x},s)|^2 + \frac{\epsilon}{2}|\theta_2(\mathbf{x},t)|^2\right)\mathrm{d}s\mathrm{d}t\mathrm{d}\mathbf{x}\\ \le{}& \sum_{K\in\mathcal{T}_h}\int_K\left(\tau\sum_{i=0}^j\int_{I_i}\frac{1}{2\epsilon}|\xi_2(\mathbf{x},s)|^2\mathrm{d}s + t_{j+1}\int_{I_j}\frac{\epsilon}{2}|\theta_2(\mathbf{x},t)|^2\mathrm{d}t\right)\mathrm{d}\mathbf{x}\\ ={}& \frac{\tau}{2\epsilon}\sum_{i=0}^j\sum_{K\in\mathcal{T}_h}\int_K||\xi_2(\mathbf{x},t)||^2_{0,I_i}\mathrm{d}\mathbf{x} + \frac{\epsilon t_{j+1}}{2}\int_{I_j}\sum_{K\in\mathcal{T}_h}\int_K|\theta_2(\mathbf{x},t)|^2\mathrm{d}\mathbf{x}\mathrm{d}t.\end{aligned}$$

Therefore we obtain an estimate for $\mathcal{A}_3^j$

$$\mathcal{A}_3^j \le C\tau^{2r+3}\sum_{i=0}^{j}\sum_{K\in\mathcal{T}_h}\int_K ||\mathbf{E}^\lambda(\mathbf{x},\cdot)||^2_{r+1,I_i}\mathrm{d}\mathbf{x} + \frac{\epsilon||\tilde{\kappa}||_\infty t_{j+1}}{2}\int_{I_j}||\theta_2(\cdot,t)||^2_{0,\mathcal{T}_h}\mathrm{d}t, \tag{3.51}$$

by using Lemma 3.2 again.

In summary, we obtain

$$\begin{aligned}\bar{\mathbf{B}}_h(\mathbf{R},\theta) \le{}& Ch^{2k+1}|||\mathbf{U}|||^2_{h,k+1,0} + C\tau^{2r+2}|||\mathbf{U}|||^2_{h,0,r+1}\\ &+C\tau^{2r+2}\Big(|||\nabla\times\mathbf{H}^\lambda|||^2_{h,0,r+1} + |||\nabla\times\mathbf{E}^\lambda|||^2_{h,0,r+1}\Big) + \frac{1}{2}\Theta_{T,\mathcal{T}_h}(\theta)\\ &+\frac{1+\lambda}{2}|||\mathbf{Q}^{1/2}\theta|||^2_h + \left(c+\frac{T\epsilon||\tilde{\kappa}||_\infty}{2}\right)|||\theta_2|||^2_h + C\tau^{2r+2}T|||\mathbf{E}^\lambda|||^2_{h,0,r+1}.\end{aligned} \tag{3.52}$$

by using the fact $n\tau = T$ and (3.43), (3.48), (3.49) and (3.51). □

Our main theoretical results will be stated in the following proposition.

Proposition 3.6 Let $\mathbf{U}_h = (\mathbf{H}_h^\lambda, \mathbf{E}_h^\lambda)^T$ be the solution of (2.14) and $(\mathbf{H},\mathbf{E})^T$ the exactly smooth solution of (2.1)-(2.2). Assume that

$$\mathbf{H},\mathbf{E}\in\left(H^{r+1}(\mathcal{I}_h;L^2(\Omega))\right)^3\bigcap\left(L^2([0,T];H^{k+1}(\mathcal{T}_h))\right)^3,\ \nabla\times\mathbf{E},\nabla\times\mathbf{H}\in\left(H^{r+1}(\mathcal{I}_h;L^2(\Omega)\right)^3$$

and $f\in L^\infty([0,T])$. Define $(\mathbf{H}_h,\mathbf{E}_h)^T = \mathrm{e}^{\lambda t}\mathbf{U}_h$, then

$$\begin{aligned}&\mu||\mathbf{H}(\cdot,T)-\mathbf{H}_h(\cdot,T^-)||_{0,\mathcal{T}_h} + \epsilon||\mathbf{E}(\cdot,T)-\mathbf{E}_h(\cdot,T^-)||_{0,\mathcal{T}_h}\\ &\le C\tau^{r+1}\left(|||\mathbf{E}|||_{h,0,r+1} + |||\mathbf{H}(\mathbf{x},t)|||_{h,0,r+1} + |||\nabla\times\mathbf{E}|||_{h,0,r+1} + |||\nabla\times\mathbf{H}|||_{h,0,r+1}\right)\\ &\quad+Ch^{k+\frac{1}{2}}\left(|||\mathbf{E}|||_{h,k+1,0} + |||\mathbf{H}|||_{h,k+1,0}\right) + Ch^{k+1}\left(||\mathbf{E}(\cdot,T)||_{k+1,\mathcal{T}_h} + ||\mathbf{H}(\cdot,T)||_{k+1,\mathcal{T}_h}\right),\end{aligned}$$

where C relies on T, but independent of τ and h.

Proof Applying (3.32) and (3.44) in (3.31) we obtain

$$\begin{aligned}&||\mathbf{Q}^{1/2}\theta(\cdot,T^-)||^2_{0,\mathcal{T}_h} + 2\lambda|||\mathbf{Q}^{1/2}\theta|||^2_h\\ &\le Ch^{2k+1}|||\mathbf{U}|||^2_{h,k+1,0} + C\tau^{2r+2}(|||\mathbf{U}|||^2_{h,0,r+1} + |||\nabla\times\mathbf{H}^\lambda|||^2_{h,0,r+1} + |||\nabla\times\mathbf{E}^\lambda|||^2_{h,0,r+1})\\ &\quad+(1+\lambda)|||\mathbf{Q}^{1/2}\theta|||^2_h + T\epsilon||\tilde{\kappa}||_\infty|||\theta_2|||^2_h + 2\left|\int_I\int_\Omega\int_0^t\kappa(t-s)\theta_2(\mathbf{x},s)\mathrm{d}s\cdot\theta_2(\mathbf{x},t)\mathrm{d}\mathbf{x}\mathrm{d}t\right|.\end{aligned} \tag{3.53}$$

According to (3.17) we know that

$$\left|\int_I\int_\Omega\int_0^t\kappa(t-s)\theta_2(\mathbf{x},s)\mathrm{d}s\cdot\theta_2(\mathbf{x},t)\mathrm{d}\mathbf{x}\mathrm{d}t\right| \le ||\tilde{\kappa}||_\infty T|||\theta_2|||^2_h \le \frac{||\tilde{\kappa}||_\infty T}{\epsilon}|||\theta|||^2_h. \tag{3.54}$$

Therefore, for suitable $\lambda > 1 + (\frac{2}{\epsilon}+1)T||\tilde{\kappa}||_\infty$ the last three terms on the right-hand side in equation (3.53) will be absorbed by the second term on the left-hand side and we have

$$\begin{aligned}||\mathbf{Q}^{1/2}\theta(\cdot,T^-)||^2_{0,\mathcal{T}_h} \le{}& Ch^{2k+1}|||\mathbf{U}|||^2_{h,k+1,0} + C\tau^{2r+2}|||\mathbf{U}|||^2_{h,0,r+1}\\ &+C\tau^{2r+2}(|||\nabla\times\mathbf{H}^\lambda|||^2_{h,0,r+1} + |||\nabla\times\mathbf{E}^\lambda|||^2_{h,0,r+1}).\end{aligned} \tag{3.55}$$

On the other hand,

$$||\mathbf{Q}^{1/2}\mathbf{R}(\cdot,T^-)||^2_{0,\mathcal{T}_h} = ||\mathbf{Q}^{1/2}\eta(\cdot,T^-)||^2_{0,\mathcal{T}_h} \le Ch^{2k+2}||\mathbf{U}(\cdot,T)||^2_{k+1,\mathcal{T}_h}. \tag{3.56}$$

By using the triangular inequality, we have

$$\begin{aligned}&\epsilon||\mathbf{E}^{\lambda}(\cdot,T)-\mathbf{E}_h^{\lambda}(\cdot,T^-)||_{0,\mathcal{T}_h}^2+\mu||\mathbf{H}^{\lambda}(\cdot,T)-\mathbf{H}_h^{\lambda}(\cdot,T^-)||_{0,\mathcal{T}_h}^2\\ \le\ & Ch^{2k+1}|||\mathbf{U}|||_{h,k+1,0}^2+C\tau^{2r+2}|||\mathbf{U}|||_{h,0,r+1}^2+Ch^{2k+2}||\mathbf{U}(\cdot,T)||_{k+1,\mathcal{T}_h}^2\\ &+C\tau^{2r+2}\left(|||\nabla\times\mathbf{H}^{\lambda}|||_{h,0,r+1}^2+|||\nabla\times\mathbf{E}^{\lambda}|||_{h,0,r+1}^2\right).\end{aligned}\tag{3.57}$$

According to the definition of $\mathbf{U}$, we know that

$$|\mathbf{H}^{\lambda}|\le|\mathbf{H}|,\quad |\mathbf{E}^{\lambda}|\le|\mathbf{E}|,\quad |\nabla\times\mathbf{H}^{\lambda}|\le|\nabla\times\mathbf{H}|,\quad |\nabla\times\mathbf{E}^{\lambda}|\le|\nabla\times\mathbf{E}|,$$

thus

$$\begin{aligned}&\epsilon||\mathbf{E}^{\lambda}(\cdot,T)-\mathbf{E}_h^{\lambda}(\cdot,T^-)||_{0,\mathcal{T}_h}^2+\mu||\mathbf{H}^{\lambda}(\cdot,T)-\mathbf{H}_h^{\lambda}(\cdot,T^-)||_{0,\mathcal{T}_h}^2\\ \le\ & Ch^{2k+1}(|||\mathbf{H}|||_{h,k+1,0}^2+|||\mathbf{E}|||_{h,k+1,0}^2)+Ch^{2k+2}\left(||\mathbf{H}(\cdot,T)||_{k+1,\mathcal{T}_h}^2+||\mathbf{E}(\cdot,T)||_{k+1,\mathcal{T}_h}^2\right)\\ &+C\tau^{2r+2}\left(|||\mathbf{H}|||_{h,0,r+1}^2+|||\mathbf{E}|||_{h,0,r+1}^2+|||\nabla\times\mathbf{H}|||_{h,0,r+1}^2+|||\nabla\times\mathbf{E}|||_{h,0,r+1}^2\right).\end{aligned}\tag{3.58}$$

Our proof will be completed by simply using the definition of $\mathbf{E}_h$, $\mathbf{H}_h$ and (2.9). □

4 Numerical Results

It is worthy to point out that similar error estimate for 2-D Maxwell equations in dispersive media can be obtained in the same way as we have done for 3-D case, by introducing the scalar and vector curl operators

$$\mathrm{curl}\mathbf{E}=\frac{\partial E_2}{\partial x}-\frac{\partial E_1}{\partial y},\quad \nabla\times H=\left(\frac{\partial H}{\partial y},-\frac{\partial H}{\partial x}\right)^T.$$

We shall give both 2D and 3D numerical examples to validate the obtained theoretical results.

4.1 Numerical models

2D model

$$\begin{cases}\mu\dfrac{\partial H_x}{\partial t}+\dfrac{\partial E_z}{\partial y}=R_1,\\ \mu\dfrac{\partial H_y}{\partial t}-\dfrac{\partial E_z}{\partial x}=R_2,\\ \epsilon\dfrac{\partial E_z}{\partial t}-\left(\dfrac{\partial H_y}{\partial x}-\dfrac{\partial H_x}{\partial y}\right)+J(E_z)=R_3,\end{cases}$$

in $\Omega=[0,1]^2$ where $J(E_z)=\epsilon\omega_p^2\int_0^t \mathrm{e}^{-(t-\tau)}E_z(\mathbf{x},\tau)\mathrm{d}\tau$. The righthand term $\mathbf{R}_i, i=1,2,3$ are chosen such that the exact solution is

$$\begin{pmatrix}H_x\\H_y\\E_z\end{pmatrix}=100\begin{pmatrix}x(1-x)(1-2y)t\mathrm{e}^{-\nu t}\\-y(1-y)(1-2x)t\mathrm{e}^{-\nu t}\\xy(1-x)(1-y)t\mathrm{e}^{-\nu(t+(x+y)/\sqrt{2})}\end{pmatrix}.$$

3D model

$$\begin{cases}\mu\dfrac{\partial\mathbf{H}}{\partial t}+\nabla\times\mathbf{E}=R_1,\\ \epsilon\dfrac{\partial\mathbf{E}}{\partial t}-\nabla\times\mathbf{H}+\mathbf{J}(\mathbf{E})=R_2.\end{cases}\tag{4.1}$$

in $\Omega = [0,1]^3$ with dispersive term $\mathbf{J}(\mathbf{E}) = \int_0^t \mathrm{e}^{-(t-\tau)}\mathbf{E}(\mathbf{x},\tau)\mathrm{d}\tau$. We choose suitable $\mathbf{R}_i, i = 1,2$ such that the exact solution is

$$\mathbf{E} = \begin{pmatrix} (y-y^2)(z-z^2) \\ (x-x^2)(z-z^2) \\ (x-x^2)(y-y^2) \end{pmatrix} t\mathrm{e}^{-(t+x+y+z)} \qquad \mathbf{H} = \begin{pmatrix} y-z \\ z-x \\ x-y \end{pmatrix} t\mathrm{e}^{-(t+x+y+z)}.$$

For simplicity we assume that $\mu = \epsilon = \nu = \omega_p = 1$.

4.2 L^2-convergence rate

In order to show the convergence rate we do the numerical calculation on a series of nested mesh, e.g., 8×8, 16×16 and 32×32 mesh respectively for 2D case. We choose the time step size $\tau = h$. The L^2-errors and their corresponding convergence rate by using our DG approach are presented in Table 1 (2D), Table 2 (2D) and Table 3 (3D), Table 4 (3D) for $r = k = 1$ and $r = k = 2$, respectively. Here N is the number of time steps, T is the time where the program stopped. Further, the optimal convergence rate is more clearly presented in Fig.1 ($r = k = 1$ 2D), Fig.2 ($r = k = 2$ 2D) and Fig.3 ($r = k = 1$ 3D), Fig.4 ($r = k = 2$ 3D). Obviously, the numerical results show a convergence rate of $O(h^{k+1})$ in space for both $\mathbf{H}_h$ and $\mathbf{E}_h$ in L^2 norm.

Table 1 The numerical results for $r = k = 1$, 2D case

time	time step	mesh	$\|\|\mathbf{E}(\cdot,T) - \mathbf{E}_h(\cdot,T^-)\|\|_{0,\Omega}$	order	$\|\|\mathbf{H}(\cdot,T) - \mathbf{H}_h(\cdot,T^-)\|\|_{0,\Omega}$	order
$T = 0.25$	$N = 2$	8×8	1.0550e-2		5.3149e-2	
	$N = 4$	16×16	2.0702e-3	2.3494	1.4267e-2	1.8973
	$N = 8$	32×32	4.5282e-4	2.1928	3.8463e-3	1.8911
$T = 0.5$	$N = 4$	8×8	2.0245e-2		1.0925e-1	
	$N = 8$	16×16	3.7030e-3	2.4508	3.1395e-2	1.7990
	$N = 16$	32×32	7.7328e-4	2.2596	8.8961e-3	1.8193
$T = 1$	$N = 8$	8×8	2.5048e-2		2.1774e-1	
	$N = 16$	16×16	5.0312e-3	2.3157	6.7556e-2	1.6885
	$N = 32$	32×32	1.0579e-3	2.2497	1.9993e-2	1.7566

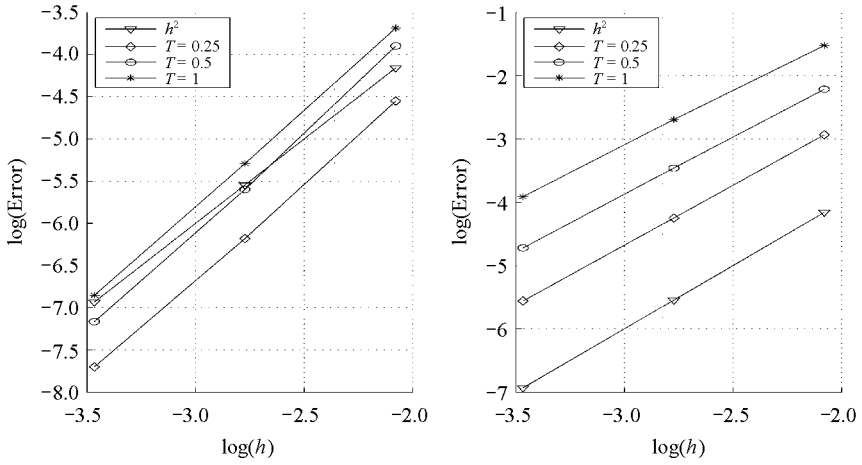

Fig.1 Convergence rate of electric field $\mathbf{E}$ (left) and magnetic field $\mathbf{H}$ (right) for $r = k = 1$ (2D case)

Table 2 The numerical results for $r = k = 2$, 2D case

time	time step	mesh	$\|\|\mathbf{E}(\cdot,T) - \mathbf{E}_h(\cdot,T^-)\|\|_{0,\Omega}$	order	$\|\|\mathbf{H}(\cdot,T) - \mathbf{H}_h(\cdot,T^-)\|\|_{0,\Omega}$	order
$T = 0.25$	$N = 2$	8×8	4.7267e-4		2.3770e-3	
	$N = 4$	16×16	5.6656e-5	3.0605	2.9847e-4	2.9935
	$N = 8$	32×32	6.9378e-6	3.0297	3.7412e-5	2.9960
$T = 0.5$	$N = 4$	8×8	7.3342e-4		3.7619e-3	
	$N = 8$	16×16	8.8213e-5	3.0556	4.7159e-4	2.9959
	$N = 16$	32×32	1.0806e-5	3.0292	5.6960e-5	3.0495
$T = 1$	$N = 8$	8×8	8.8998e-4		4.9033e-3	
	$N = 16$	16×16	1.0709e-4	3.0549	6.1096e-4	3.0046
	$N = 32$	32×32	1.3116e-5	3.0294	7.5816e-5	3.0105

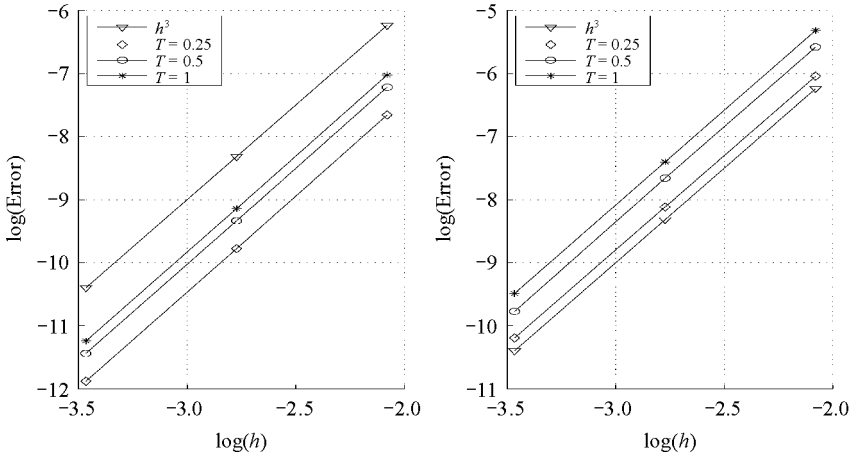

Fig.2 Convergence rate of electric field $\mathbf{E}$ (left) and magnetic field $\mathbf{H}$ (right) for $r = k = 2$ (2D case)

Table 3 The numerical results for $r = k = 1$, $h = \tau$, 3D case

time	time step	mesh	$\|\|\mathbf{E}(\cdot,T) - \mathbf{E}_h(\cdot,T^-)\|\|_{0,\mathcal{T}_h}$	rate	$\|\|\mathbf{H}(\cdot,T) - \mathbf{H}_h(\cdot,T^-)\|\|_{0,\mathcal{T}_h}$	rate
$T = 0.25$	$N = 1$	$4 \times 4 \times 4$	8.7992e-2		1.0410e-1	
	$N = 2$	$8 \times 8 \times 8$	2.2342e-2	1.9776	2.2670e-2	2.1991
	$N = 4$	$16 \times 16 \times 16$	5.5970e-3	1.9970	6.8822e-3	1.7198
$T = 0.5$	$N = 2$	$4 \times 4 \times 4$	1.4592e-1		1.6426e-1	
	$N = 4$	$8 \times 8 \times 8$	3.6730e-2	1.9901	4.9850e-2	1.7203
	$N = 8$	$16 \times 16 \times 16$	9.1150e-3	2.0106	1.1863e-2	2.0711
$T = 1$	$N = 4$	$4 \times 4 \times 4$	1.8611e-1		2.1165e-1	
	$N = 8$	$8 \times 8 \times 8$	4.7487e-2	1.9706	6.0191e-2	1.8141
	$N = 16$	$16 \times 16 \times 16$	1.2009e-2	1.9834	1.7893e-2	1.7502

Table 4 The numerical results for $r = k = 2$, $h = \tau$, 3D case

time	time step	mesh	$\|\|\mathbf{E}(\cdot,T) - \mathbf{E}_h(\cdot,T^-)\|\|_{0,\mathcal{T}_h}$	rate	$\|\|\mathbf{H}(\cdot,T) - \mathbf{H}_h(\cdot,T^-)\|\|_{0,\mathcal{T}_h}$	rate
$T = 0.25$	$N = 1$	$4 \times 4 \times 4$	6.8566e-5		6.7509e-5	
	$N = 2$	$8 \times 8 \times 8$	8.7785e-6	2.9654	9.0006e-6	2.9070
	$N = 4$	$16 \times 16 \times 16$	1.1314e-6	2.9559	1.1825e-6	2.9282
$T = 0.5$	$N = 2$	$4 \times 4 \times 4$	1.1202e-4		1.0936e-4	
	$N = 4$	$8 \times 8 \times 8$	1.4303e-5	2.9694	1.4438e-5	2.9211
	$N = 8$	$16 \times 16 \times 16$	1.8841e-6	2.9244	1.9333e-6	2.9007
$T = 1$	$N = 4$	$4 \times 4 \times 4$	1.4472e-4		1.4083e-4	
	$N = 8$	$8 \times 8 \times 8$	1.8648e-5	2.9562	1.8525e-5	2.9264
	$N = 16$	$16 \times 16 \times 16$	2.4222e-6	2.9446	2.5589e-6	2.8559

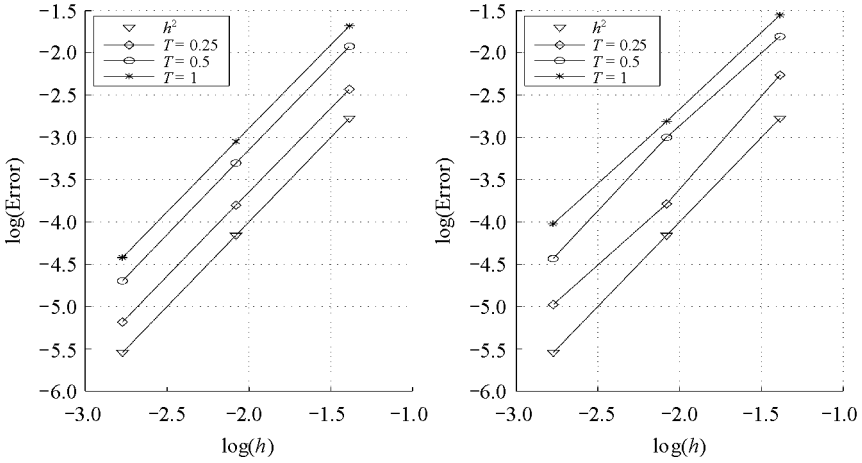

Fig.3 Convergence rate of $\mathbf{E}$ (left) and $\mathbf{H}$ (right) for $r = k = 1$ (3D case)

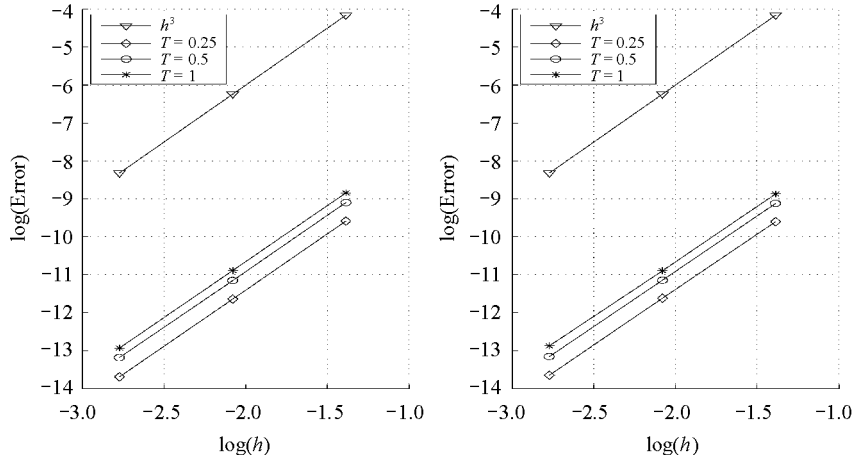

Fig.4 Convergence rate of $\mathbf{E}$ (left) and $\mathbf{H}$ (right) for $r = k = 2$ (3D case)

4.3 The ultra-convergence of order $2r + 1$ in time variable t

Although the theoretical error bound is $O(h^{k+1/2} + \tau^{r+1})$, our numerical experiments indicates that the actual error bound seems to be $O(h^{k+1/2} + \tau^{2r+1})$. Here, we only use the 3-D example to illustrate this phenomenon. First, we choose $\tau = h$ but use polynomial space $(\mathcal{P}^2)^3 \times \mathcal{P}^1$. Corresponding L^2-error and convergence rate are listed in Table 5. Apparently, we

have convergence rate of $O(h^3)$. Then we use polynomial spaces $(\mathcal{P}^r)^3 \times \mathcal{P}^r$, but let $\tau^2 = h$ and list the numerical results in Table 6. We can see that convergence rates of $O(\tau^3)$ and $O(\tau^5)$ is obtained for $r = 1$ and $r = 2$, respectively.

Table 5 The numerical results for $r = 1$, $k = 2$

time	time step	mesh	$\|\|\mathbf{E}(\cdot,T) - \mathbf{E_h}(\cdot,T^-)\|\|_{0,\mathcal{T}_h}$	rate	$\|\|\mathbf{H}(\cdot,T) - \mathbf{H_h}(\cdot,T^-)\|\|_{0,\mathcal{T}_h}$	rate
$T = 0.25$	$N = 1$	$4 \times 4 \times 4$	3.3139e-4		2.3061e-4	
	$N = 2$	$8 \times 8 \times 8$	4.7340e-5	2.8074	3.4306e-5	2.7489
	$N = 4$	$16 \times 16 \times 16$	6.2757e-6	2.9152	4.6453e-6	2.8846
$T = 0.5$	$N = 2$	$4 \times 4 \times 4$	3.7585e-4		1.9532e-4	
	$N = 4$	$8 \times 8 \times 8$	5.1260e-5	2.8743	2.9949e-5	2.7053
	$N = 8$	$16 \times 16 \times 16$	6.6880e-6	2.9382	4.2460e-6	2.8183
$T = 1$	$N = 4$	$4 \times 4 \times 4$	1.6655e-4		2.9135e-4	
	$N = 8$	$8 \times 8 \times 8$	2.5030e-5	2.7342	4.3015e-5	2.7598
	$N = 16$	$16 \times 16 \times 16$	3.7117e-6	2.7535	5.7338e-6	2.9073

5 Concluding Remarks

In this paper, we investigate a space-time DG method for solving Maxwell's equations in dispersive media. Both the L^2-stability and error estimate of rate $O(\tau^{r+1} + h^{k+\frac{1}{2}})$ are obtained. Furthermore, our approach has great flexibility, non-uniform mesh and polynomials of different degrees can be employed in this method. Hence, an hp-version DG method and its corresponding analysis will be our ongoing work. Numerical examples are given to validate the theoretical predictions. Moreover, the numerical results show a $2r + 1$ order ultra-convergence of the numerical flux in time variable t at grid points. That is, for the errors $\|\mathbf{E}(\cdot,t_j) - \mathbf{E}_h(\cdot,t_j^-)\|_{0,\mathcal{T}_h}$ and $\|\mathbf{H}(\cdot,t_j) - \mathbf{H}_h(\cdot,t_j^-)\|_{0,\mathcal{T}_h}$, we believe that the convergence rate should be $O(\tau^{2r+1} + h^{k+1})$, when polynomials of degree at most r and k are used in temporal and spatial discretization, respectively.

Table 6 The ultra-convergence of order $2k + 1$ in t, $r = k$, $h = \tau^2$, $T = 1$

k	τ	mesh	$\|\|\mathbf{E}(\cdot,T) - \mathbf{E_h}(\cdot,T^-)\|\|_{0,\mathcal{T}_h}$	rate	$\|\|\mathbf{H}(\cdot,T) - \mathbf{H_h}(\cdot,T^-)\|\|_{0,\mathcal{T}_h}$	rate
1	$\frac{1}{2}$	$4 \times 4 \times 4$	1.9041e-1		2.4251e-1	
	$\frac{1}{4}$	$16 \times 16 \times 16$	1.4762e-2	3.6891	3.1335e-2	2.9522
2	$\frac{1}{2}$	$4 \times 4 \times 4$	1.6086e-4		1.4707e-4	
	$\frac{1}{4}$	$16 \times 16 \times 16$	3.4978e-6	5.5232	3.6261e-6	5.3419

References

[1] Argyris J H, Scharpf D W. Finite elements in time and space. Nucl Engrg Des, 1969, **10**: 456–464

[2] Bonnerot R, Jamet P. Numerical computation of the free boundary for the two-dimensional Stefan problem by space-time finite elements. J Comput Phys, 1977, **25**: 163–181

[3] Bruch J C, Zyvoloski G. Transient two-dimensional heat conduction problems solved by the finite element method. Int J Numer Methods Engrg, 1974, **8**: 481–494

[4] Castillo P, Cockburn B, Schötzau D, et al. Optimal a priori error estimates for the *hp*-version of the local discontinous Galerkin method for convection-diffusion problems. Math Comp, 2001, **71**: 455–478

[5] Cella A, Lucchesi M. Space-time finite elements for the wave propagation problem. Meccanica, 1975, **10**: 168–170

[6] Chen C M. Structure Theory of Superconvergence of Finite Elements. Changsha: Hunan Science and Technology Press, 2001

[7] Chen M H, Cockburn B, Reitich F. High-order RKDG methods for computational electromagnetics. J Sci Comput, 2005, **22/23**: 205–226

[8] Ciarlet Jr P, Zou J. Fully discrete finite element approaches for time-dependent Maxwell equations. Numer Math, 1999, **82**: 193–219

[9] Cockburn B, Li F, Shu C W. Locally divergence-free discontinuous Galerking methods for the Maxwell equations. J Comput Phys, 2004, **194**: 588–610

[10] Douglas T, Dupont T, Wheeler M F. An L^∞ estimate and superconvergence result for a Galerkin method for elliptic equations based on tensor products of piecewise polynomials. RAIRO Anal Numer, 1974, **8**: 61–66

[11] Fried I. Finite element analysis of time-dependent phenomena. AIAA J, 1969, **7**: 1170–1173

[12] Hesthaven J S, Warburton T. Nodal high-order methods on unstructured grids. I. Time-domain solution of Maxwell equations. J Comput Phys, 2002, **181**: 186–221

[13] Hughes T J R, Hulbert G M, Space-time finite element methods for elastodynamics: formulations and error estimates. Comput Methods Appl Mech Engrg, 1988, **66**: 339–363

[14] Lee R L, Madsen N K. A mixed finite element formulation for Maxwell's equations in the time domain. J Comput Phys, 1990, **88**: 284–304

[15] Lesaint P, Raviart P A. On a finite elment method for solving the neutron transport equation//deBoor C. ed. Mathematical Aspects of Finite Elements in Partial Differential Equations New York: Academic Press, 1974: 89–123

[16] Li J. Error analysis of fully discrete mixed finite element schemes for 3-D Maxwell's equations in dispersive media. Comput Methods Appl Mech Engrg, 2007, **196**: 3081–3094

[17] Li J. Error analysis of finite element methods for 3-D Maxwell's equations in dispersive media. J Comput Appl Math, 2006, **188**: 107–120

[18] Li J, Chen Y. Analysis of a time-domain finite element method for 3-D Maxwell's equations in dispersive media. Comput Methods Appl Mech Engrg, 2006, **195**: 4220–4229

[19] Li J, Wood A. Finite element analysis for wave propagation in double negative metamaterials. J Sci Comput, 2007, **32**(2): 263–284

[20] Lu T, Zhang P, Cai W. Discontinuous Galerkin methods for dispersive and lossy Maxwell's equations and PML boundary conditions. J Comput Phys, 2004, **200**: 549–580

[21] Johnson C. Error estimates and automatic time step control for numerical methods for stiff ordinary differential equations, Technical Report 1984-27, Department of Mathematics, Chalmers University of Technology and University of Göteborg, Göteborg, Sweden, 1984

[22] Ma C F. Finite-element method for time-dependent Maxwell's equations based on an explicit-magnetic-field scheme. J Comput and Appl Math, 2006, **194**: 409–424

[23] Makridakis C G, Monk P. Time-discrete finite element schemes for Maxwell's equations. RAIRO Math Modeling Numer Anal, 1995, **29**: 171–197

[24] Monk P. Anlysis of a finite element method for maxwell's equations. SIAM J Numer Anal, 1992, **29**(3): 714–729

[25] Nédélec J C. A new family of mixed finite elements in $\mathcal{R}^3$. Numer Math, 1986, **50**: 47–81

[26] Oden J T. A general theory of finite elements II. Applications. Int J Numer Methods Engrg, 1969, **1**: 247–259

[27] Reed W H, Hill T R. Triangular mesh methods for the neutron transport equation. Report LA-UR-73479, Los Alamos Scientific Laboratory, Los Alamos, 1973

[28] Wang B, Xie Z Q, Zhang Z M. Error analysis of a discontinuous Galerkin method for Maxwell equations in dispersive media. J Comput Phys, 2010, **229**: 8552–8563

[29] Wang B, Xie Z Q, Zhang Z M. Space-time discontinuous Galerkin method for Maxwell equations. Commun Comput Phys, 2013, **14**(4): 916–939

[30] Yee K S. Numerical solution of initial boundary value problems involving Maxwell's equations in isotropic media. IEEE Trans Antennas Propagat, 1966, **14**: 302–307